Renewable Energy 41 (2012) 254–261

Contents lists available at SciVerse ScienceDirect

Renewable Energy

journal homepage: www.elsevier.com/locate/renene

System simulation of a linear concentrating photovoltaic system with an active cooling system

Tony Kerzmann [a,*], Laura Schaefer [b]

[a] Swanson School of Engineering, 341 Benedum Hall, University of Pittsburgh, Pittsburgh, PA 15261, USA
[b] Swanson School of Engineering, 153 Benedum Hall, University of Pittsburgh, Pittsburgh, PA 15261, USA

ARTICLE INFO

Article history:
Received 18 August 2010
Accepted 5 November 2011
Available online 3 December 2011

Keywords:
Linear concentrating photovoltaic
CPV
Solar thermal
Linear Fresnel lens
Multijunction cell
Concentrating PV/T system

ABSTRACT

Recent interest in concentrating photovoltaics (CPV) have led to research and development of multiple CPV systems throughout the world. Much of the focus has been on 3D high concentration systems without cell cooling. This research makes use of a system simulation to model a medium 2D solar concentration energy system with an active cooling system. The simulation encompasses the modeling of a GaInP/GaAs/Ge triple-junction solar cell, the fluid and heat transfer properties of the cooling system, and the storage tank. The simulation was coded in Engineering Equation Solver and was used to simulate the linear concentrating photovoltaic system (LCPV) under Phoenix, AZ, solar and climactic conditions for a full year. The output data from this simulation was used to evaluate the LCPV system from an economic and environmental perspective, showing that over one year a 6.2 kWp LCPV system would save a residential user $1623 in electricity and water heating, as well as displace 10.35 tons of CO_2.

1. Introduction

Because of their high electricity conversion efficiencies, multijunction cells have seen a significant increase in research interest and research funding over the last ten years. PV cell manufacturing techniques have improved in recent years, assisting in higher material purity and less material defects. As these techniques improve, so too do the efficiencies of the multijunction cells. Of the different solar cell technologies, the multijunction concentrator cells have demonstrated the greatest increases in efficiency, reaching a record breaking 41.1% [1]. Because of their high efficiency, multijunction cells have one of the largest potentials for decreased solar energy production costs now and in the future. In order to be cost effective, these systems must have a concentration system, and therefore must also have a solar tracking system. Further efficiency gains can be accomplished by including a cooling system to reduce the cell temperature. As solar cells increase in temperature, the cell efficiency decreases. This decrease can have adverse effects on the cell efficiency and therefore power output at medium and high concentration levels.

This research focuses on the young and growing field of concentrating PV systems, specifically that of linear concentrating systems that use high efficiency multijunction cells. The linear concentrating photovoltaic system (LCPV) system that was simulated combines a linear Fresnel lens, high efficiency GaInP/GaAs/Ge cells, and a fluid cooling channel. A conceptual drawing of this system can be seen in Fig. 1, where the solar radiation is focused onto the multijunction cells and the heat is removed using an active cooling system.

The cooling system is used to cool the cells so that higher cell efficiencies can be maintained, and the excess heat that is withdrawn from the module is then stored and used as a heat source. Fig. 2 gives a heat flow example of how this heat would be extracted and stored in a system designed for residential use. When the LCPV system receives solar radiation, the pump turns on, constantly circulating the fluid from the storage tank. The fluid in the tank heats up, and can be used for heating purposes. The hot fluid produced by the LCPV system can thereby partially or fully displace the energy consumption associated with hot water generation in a residential home, for instance.

A three-dimensional drawing of the LCPV system as it would look in service with a tracking system is shown in Fig. 3. This drawing represents a 6.2 kWp system under standard test conditions of 1000 W/m^2 solar radiation and 25 °C ambient temperature. The drawing does not include the entering and exiting fluid piping

* Corresponding author. Tel.: +1 412 478 1670.
E-mail addresses: tonykerz@yahoo.com (T. Kerzmann), laschaef@engr.pitt.edu (L. Schaefer).

0960-1481/$ – see front matter
doi:10.1016/j.renene.2011.11.004

Nomenclature

η_{cell}	efficiency
$\overline{\eta}_{cell}$	average efficiency
κ	thermal conductivity (kW/m·K)
κ_{liquid}	thermal conductivity of fluid in liquid state (kW/m·K)
μ	dynamic viscosity (kg/m·s)
ν	kinematic viscosity (m^2/s)
ρ	density (kg/m^3)
$\rho_{citywater}$	density of city water (kg/m^3)
ρ_{gas}	density of fluid in gas state (kg/m^3)
ρ_{liquid}	density of fluid in liquid state (kg/m^3)
$\rho_{tank,i-1}$	density of the fluid in the tank from the previous hourly iteration (kg/m^3)
$A_{cross-section}$	cross-sectional area ofkW/m·K the flow channel (m^2)
$A_{surface}$	outside surface area of the flow channel (m^2)
Bo	boiling number
Co	convection number
Cp	specific heat (kJ/kg·K)
D_h	hydraulic diameter (m)
$E_{citywater}$	thermal energy of city water flowing into the storage tank (kJ)
E_{in}	thermal energy flowing from the channel to the storage tank (kJ)
E_{loss}	thermal energy leaving the storage tank through conduction (kJ)
E_{out}	thermal energy flowing from the storage tank to the channel (kJ)
E_{tank}	thermal energy in the storage tank (kJ)
E_{use}	thermal energy leaving the storage tank for use (kJ)
f	friction factor
Fr_{liquid}	Froude number of fluid in liquid state
G	mass flux (kg/m^2·s)
h_{bulk}	enthalpy of fluid bulk flow (kJ/kg)
$h_{bulk,i-1}$	enthalpy of fluid bulk flow from previous channel segment (kJ/kg)
$h_{citywater}$	enthalpy of the city water (kJ/kg·K)
h_{fg}	change in enthalpy from gas to liquid state in fluid (kJ/kg)
h_{gas}	enthalpy of fluid in the gas state (kJ/kg)
h_{heat}	enthalpy entering the fluid in the flow channel (kJ/kg)
h_{liquid}	enthalpy of fluid in the liquid state (kJ/kg)
ht	heat transfer coefficient (kW/m^2·K)
$\overline{ht}$	average heat transfer coefficient (kW/m^2·K)
ht_i	heat transfer coefficient at channel segment i (kW/m^2·K)
ht_{CBD}	convective-boiling-dominant heat transfer coefficient (kW/m^2·K)
ht_{liquid}	heat transfer coefficient of fluid in liquid state (kW/m^2·K)
ht_{NBD}	nucleate-boiling-dominant heat transfer coefficient (kW/m^2·K)
h_{tank}	enthalpy of the fluid in the storage tank (kJ/kg·K)
$h_{tank,i}$	enthalpy of the fluid in the storage tank at channel segment i (kJ/kg·K)
Length	module length (m)
$\dot{m}$	mass flow rate (kg/s)
$Mass_{tank}$	mass of the fluid in the storage tank (kg)
Nu	Nusselt number
p	perimeter of the flow channel cross-section (m)
P_{Cell}	LCPV system power (kW)
Pr	Prandtl number
Pr_{liquid}	Prandtl number of fluid in liquid state
$\ddot{q}_{heat}$	heat flux entering the fluid from the solar radiation (kW/m^2)
$\ddot{q}_{rad}$	solar radiation (kW/m^2)
q_{total}	heat entering the flow channel (kW)
$R_{channel}$	thermal resistance of the flow channel insulation (kW/K·m^2)
R_{tank}	thermal resistance of the storage tank insulation (kW/K·m^2)
Re	Reynolds number
Re_{liquid}	Reynolds number of fluid in liquid state
Rows	number of module rows in the LCPV array
$SurfaceArea_{tank}$	surface area of the storage tank (m^2)
T_{air}	outdoor air temperature (K)
T_{bulk}	temperature of the bulk fluid flow in the channel (K)
$\overline{T}_{bulk}$	average temperature of the bulk fluid flow in the channel (K)
$T_{bulk,i}$	temperature of the bulk fluid flow in channel segment i (K)
T_{room}	indoor air temperature (K)
$\overline{T}_{surface}$	average channel surface temperature (K)
T_{tank}	temperature of the fluid in the storage tank (K)
U_{liquid}	velocity of the fluid in liquid state (m/s)
U_m	average velocity of the fluid flow in the channel (m/s)
V_{use}	volume of fluid that leaves system due to use (m^3)
$Width_{concentration}$	width of the concentration area (m)

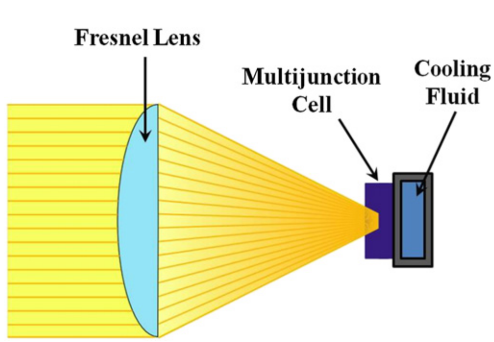

Fig. 1. Component Drawing of the Linear Concentrating Photovoltaic System.

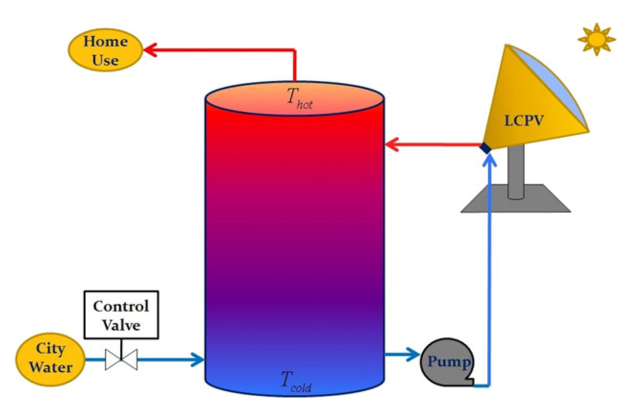

Fig. 2. LCPV System with Flow Diagram.